Journal of Power Sources 196 (2011) 5853–5857

Contents lists available at ScienceDirect

Journal of Power Sources

journal homepage: www.elsevier.com/locate/jpowsour

Short communication

Performance of Au and AuAg nanoparticles supported on Vulcan in a glucose laminar membraneless microfuel cell

F.M. Cuevas-Muñiz [b], M. Guerra-Balcázar [a], F. Castaneda [a], J. Ledesma-García [b,*], L.G. Arriaga [a,**]

[a] Centro de Investigación y Desarrollo Tecnológico en Electroquímica, 76703 Querétaro, Mexico
[b] División de Investigación y Posgrado, Facultad de Ingeniería, Universidad Autónoma de Querétaro, 76010 Querétaro, Mexico

ARTICLE INFO

Article history:
Received 5 January 2011
Received in revised form 25 February 2011
Accepted 28 February 2011
Available online 8 March 2011

Keywords:
Au nanoparticles
AuAg alloy
Microfluidic fuel cell
Glucose oxidation

ABSTRACT

Au and AuAg electrocatalysts were prepared by chemical reduction and supported on Vulcan XC-72 for their application in a laminar membraneless microfluidic fuel cell that operates with glucose as fuel in basic media. Average particle size and lattice parameters were determined by X-ray diffraction technique, resulting in 4 and 21 nm for Au and AuAg respectively. The composition ratio of Au and Ag in the mixture was estimated by X-ray fluorescence. X-ray photoelectron spectroscopy measurements were used to determinate oxidation states. The electrocatalytic activity of Au/C and AuAg/C materials was investigated in terms of glucose electrooxidation in 0.3 M KOH. The results obtained by electrochemical studies in a half cell configuration showed that the onset potential for glucose oxidation on AuAg/C presented a negative shift ca. 150 mV compared with Au/C. AuAg/C was evaluated in a microfluidic fuel cell operated with glucose as fuel showing good stability and higher performance when was compared with Au/C.

1. Introduction

In the last few years, the energy demand is constantly growing. Several fuels have been widely studied due to their potential utilization in energy conversion systems such as formic acid, glycerol, ethylene glycol and glucose [1–4]. The main reason is related with their low toxicity, facility of storage and environmentally friendly.

In this context, glucose, molecule abundant in nature and whose theoretical energy density is comparable with methanol, has shown potential applications in small portable fuel cell applications [4,5]. A primary advantage of glucose oxidation reaction is the formation of non-toxic products (water and CO_2). However in the practice, the reaction is incomplete by the production of gluconate/gluconic acid, which reduces the performance obtained by glucose-based fuel cell [6]. Other disadvantage is the low performance in electrochemical cells due to slow kinetics and poisoning effect by reaction products on electrode surface.

Some studies have shown for instance that Au and Ag catalysts have ability to carry out the glucose oxidation reaction [7–11]. Yet, it has already been reported that AuAg bimetallic nanoparticles exhibit good electrochemical activity for glucose oxidation, therefore they have been used in order to increase the fuel cell performance and to reduce catalyst cost [12,13].

There are some studies where glucose is used as fuel and enzymes as catalysts; however the obtained power densities are in the order of μW. Yet, we previously reported the state of the art of glucose-based fuel cells where it was compared the performance, materials and characteristics of fuel cells and microfluidic fuel cells [4].

In this context, laminar membraneless microfluidic fuel cells (LMMFC) are a kind of devices that operate without a physical barrier or membrane to separate the anode and cathode [4,14,15]. The reagents are introduced at the inlet of the micro-channel and the electrodes are placed at the opposite walls to complete the microfluidic fuel cell configuration. The absence of membrane allows the manufacture of smaller devices for specific mobile applications or medical instruments [16].

Above described represents significant advantages of LMMFC compared to proton exchange membrane fuel cells, where problems such as design, membrane cost or microfabrication difficulties limit their commercial use [17].

Hence, in this study AuAg nanoparticles supported on Vulcan carbon material were prepared and characterized by physicochemical and electrochemical techniques. AuAg/C material was used as anode electrode in LMMFC that operates with glucose as fuel. AuAg/C is used as an electrode for the first time in a LMMFC, showing stability and higher performance compared with Au/C, used as a reference.

* Corresponding author. Tel.: +52 442 1921200x65411; fax: +52 1921299x6016.
** Corresponding author. Tel.: +52 442 211 6069; fax: +52 442 211 6007.
E-mail addresses: janet.ledesma@uaq.mx (J. Ledesma-García), larriaga@cideteq.mx (L.G. Arriaga).

0378-7753/$ – see front matter © 2011 Elsevier B.V. All rights reserved.
doi:10.1016/j.jpowsour.2011.02.081

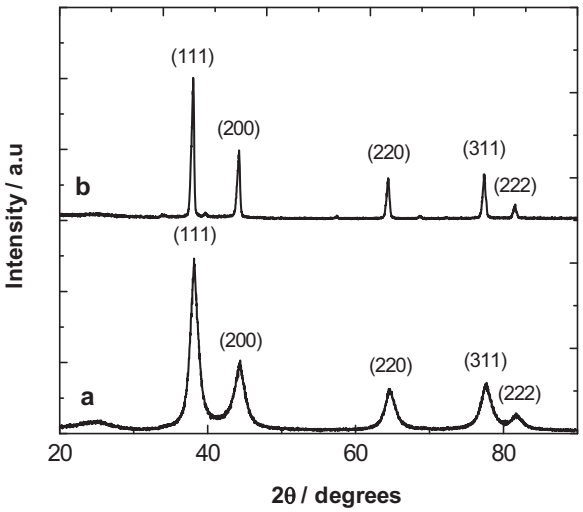

Fig. 1. XRD patterns of (a) Au/C and (b) AuAg/C.

2. Experimental

2.1. Synthesis of AuAg/C and Au/C electrocatalysts

AuAg nanoparticles were synthesized by chemical reduction in the presence of $NaBH_4$ (99.9%, Aldrich) as reducing agent. 0.25 mM $HAuCl_4{\cdot}3H_2O$ and 0.063 mM $AgNO_3$ (J.T. Baker) aqueous solutions were added to tetra-octyl-ammonium bromide (TOAB, 98% Fluka) in toluene (99.98% Aldrich) as phase-transfer agent. Dodecanethiol (98%, Aldrich) was incorporated to this solution, followed by the addition of $NaBH_4$ in excess. The reaction was maintained under constant stirring at 2 °C for 2.5 h. After that time, the solid was separated and washed with plenty ethanol (J.T. Baker) in order to be purified. Au nanoparticles were synthesized by the same procedure using 0.31 mM $HAuCl_4{\cdot}3H_2O$ [15].

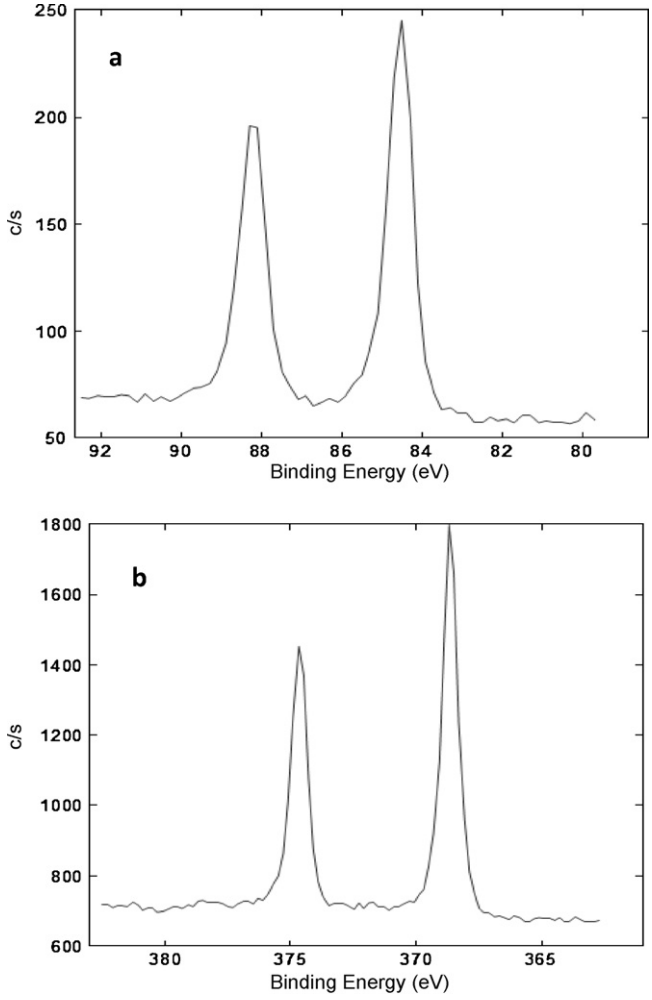

Fig. 2. X-ray photoelectron peaks for AuAg/C (a) Au 4f and (b) Ag 3d spectral region.

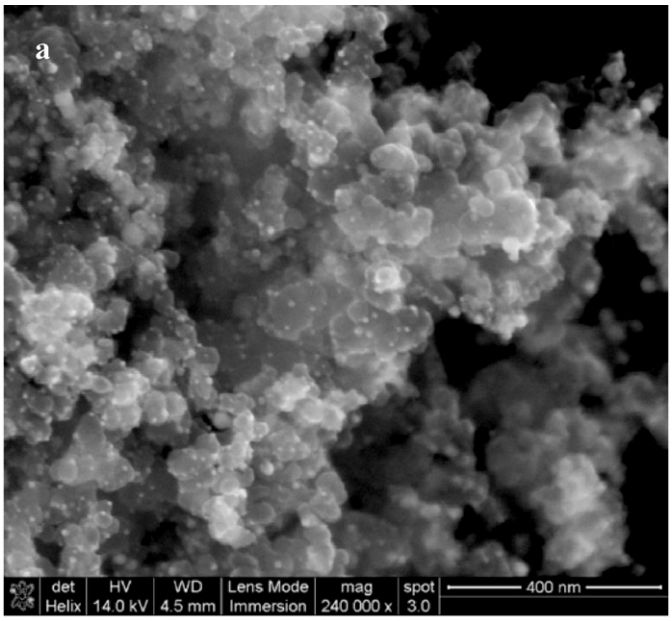

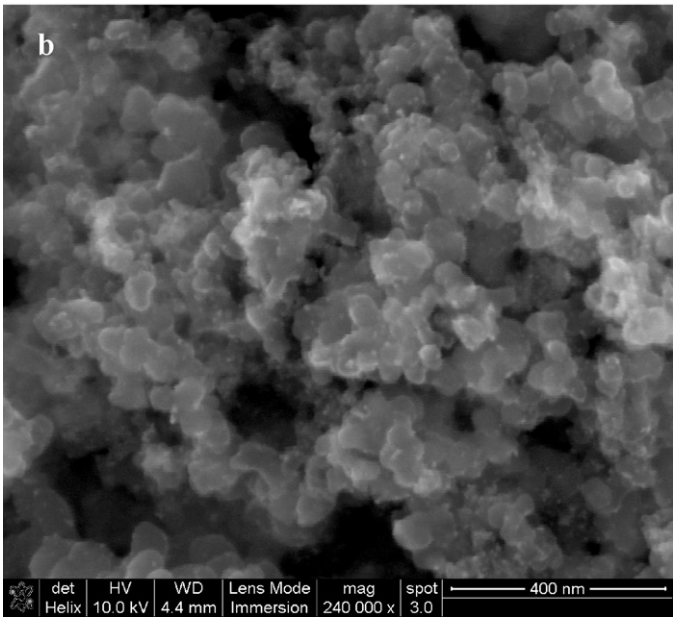

Fig. 3. SEM images of (a) Au/C and (b) AuAg/C.

The resulting nanoparticles were dispersed in hexane (99.7%, J.T. Baker) and supported by the impregnation method on XC-72 Vulcan 30:70 (w/w) ratio. Successively, they underwent a thermal treatment at 300 °C for 3 h.

2.2. Physicochemical characterization of AuAg/C and Au/C

The obtained materials were characterized by X-ray diffraction (XRD) on an X-pert MPD Phillips diffractometer using

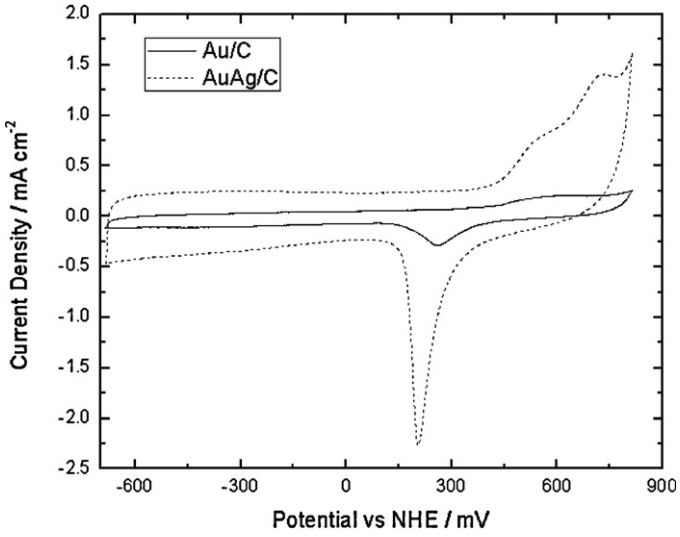

Fig. 4. Cyclic voltammograms of (a) Au/C and (b) AuAg/C electrodes in N_2-satured 0.3 M KOH. Scan rate 20 mV s^{-1} at room temperature.

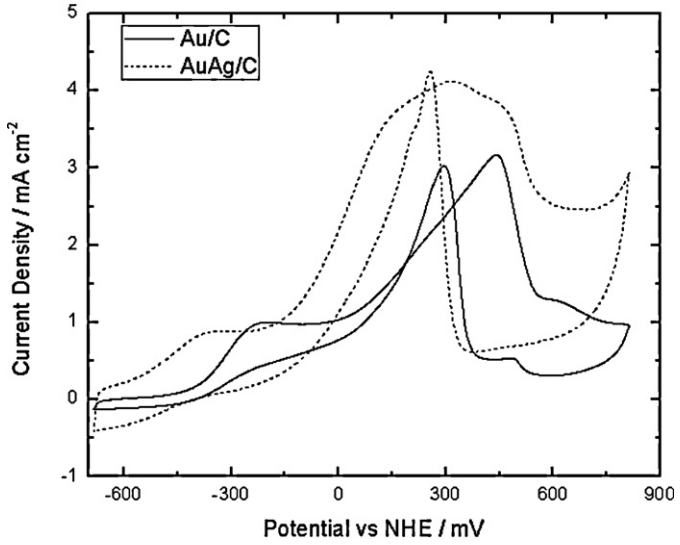

Fig. 5. Cyclic voltammograms obtained on the Au/C and AuAg/C electrodes in 0.01 M glucose + 0.3 M KOH aqueous solution at 20 mV s^{-1}.

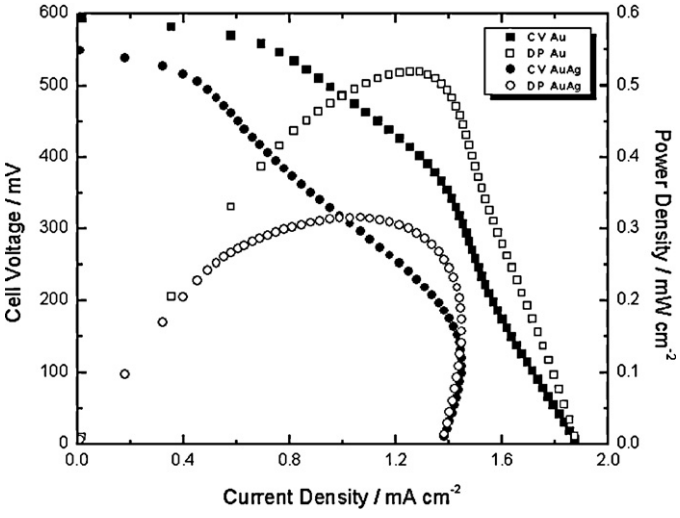

Fig. 6. Polarization and power density curves in 0.01 M glucose + 0.3 M KOH for LMMFC equipped with Au/C and AuAg/C anode electrodes at 20 mV s^{-1}.

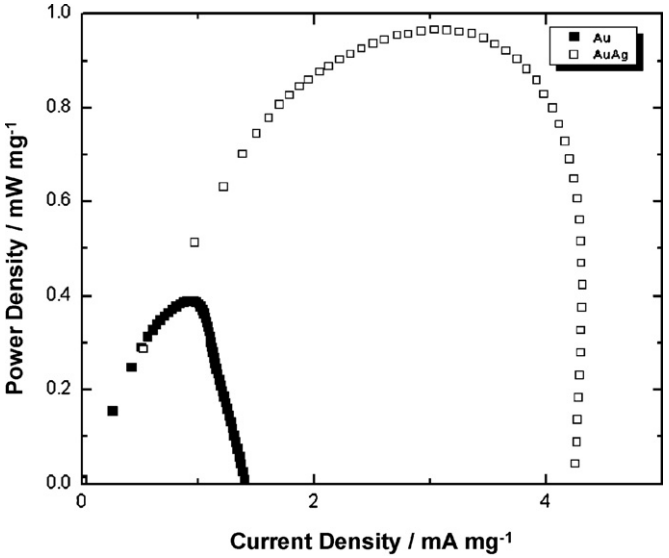

Fig. 7. Comparison of power density curves normalized by Au loading for 0.01 M glucose + 0.3 M KOH for LMMFC equipped with Au/C and AuAg/C anode electrodes at 20 mV s^{-1}.

Cu Kα radiation operating at 43 kV and 30 mA. X-ray fluorescence (XRF) analysis of the electrocatalysts was carried out by a Bruker AXS S4 Explorer spectrometer operating at 1 kW and equipped with Rh X-ray source, an LiF 220 crystal analyzer, and a 0.12° divergence collimator. X-ray photoelectron spectroscopy (XPS) measurements were performed by using a Physical Electronics (PHI) 5800-01 spectrometer. A monochromatic Al Kα X-ray source was used at 350 W. A Nova nano-SEM 200 FEI high resolution scanning electron microscope (HR-SEM) on the other hand, was used to investigate the catalysts morphology.

2.3. Electrochemical evaluation of AuAg/C and Au/C

Electrochemical experiments consisted in cyclic voltammetry (CV) and chronoamperometry (CA) using a BAS Epsilon Potenciostat/Galvanostat (Bioanalytical Systems). A Hg/HgO electrode (Radiometer®) and a Pt wire as reference and counter electrode respectively, were used in a standard three-electrode glass cell.

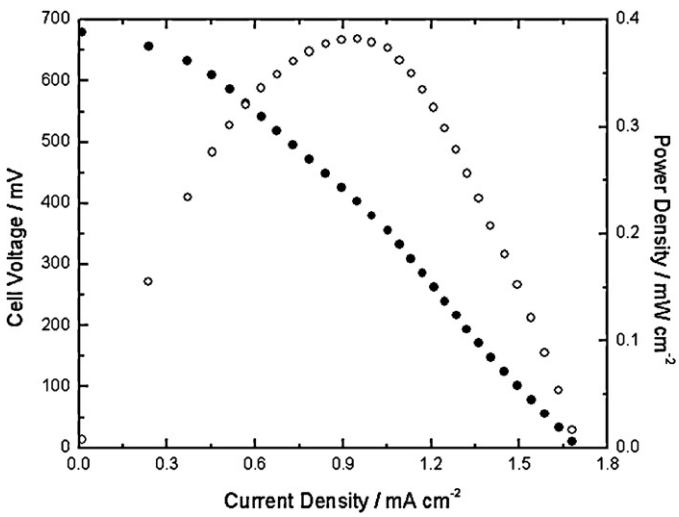

Fig. 8. Polarization and power density curve in 0.05 M glucose + 0.3 M KOH on AuAg/C anode electrode. Scan rate 20 mV s^{-1}.

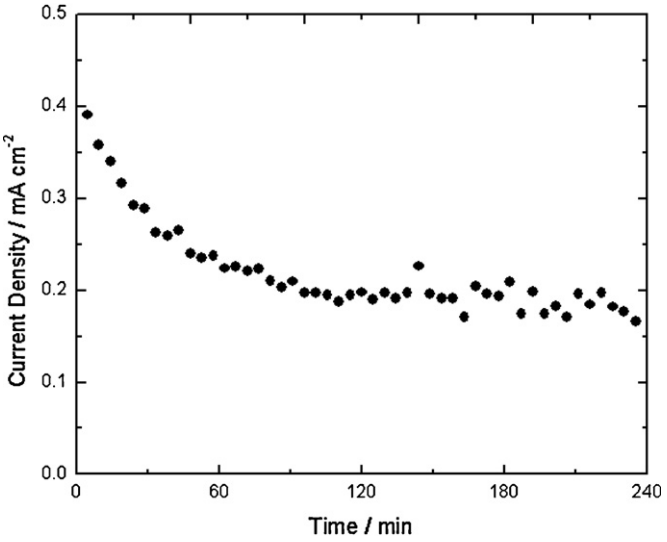

Fig. 9. Chronoamperometric curve on AuAg/C electrode at 320 mV vs. NHE for 4 h in the presence of 0.05 M glucose + 0.3 M KOH.

Potentials in the text are referred to the NHE (normal hydrogen electrode).

Working electrodes were prepared with inks of AuAg/C and Au/C. The electrocatalysts were dispersed in isopropyl alcohol and Nafion® 5% in an ultrasonic bath in 1:73:7 ratio respectively. Subsequently, the inks (0.265 mg cm^{-2} catalyst loading) were deposited onto glassy carbon electrodes (0.071 cm^2 geometric area) previously polished until mirror-finished and dried under nitrogen flow. 0.3 M KOH was used as electrolyte. All solutions were prepared with deionized DI water ($\rho \geq 18$ MΩ cm).

2.4. Microfluidic fuel cell evaluation

Microfluidic fuel cell setup reported by Morales-Acosta et al. was used [15]. Two similar microfuel cells were constructed (one for each electrocatalyst). 2 and 4 mg cm^{-2} of AuAg/C and Au/C respectively, were deposited in the anodic compartment using the spray technique. Pt/V XC-72 (30 wt.%, E-TEK) was used as catalyst in the cathodic compartment in both cells with Pt loading of 2 mg cm^{-2}. The current collectors were connected with aluminum foil to the cell. Alkaline solution of 0.05 M glucose in 0.3 M KOH was passed through the anode with a flow rate of 0.115 mL min^{-1}. Cathodic compartment is fed with 0.3 M KOH alkaline solution previously saturated with oxygen using a saturation tower, at 0.319 mL min^{-1} of flow rate.

Polarization curves were recorded at 20 mV s^{-1}. In order to evaluate the stability of AuAg/C material in the LMMFC, chronoamperometry experiments at 320 mV were carried out in the presence of 0.05 M glucose in 0.3 M KOH aqueous solution for 4 h. The experiments were carried out at room temperature.

3. Results and discussion

3.1. Physicochemical characterization

X-ray diffraction patters collected from Au/C are presented in Fig. 1a. The signals correspond to Au crystalline planes (1 1 1), (2 0 0), (2 2 0), (3 1 1) and (2 2 2) located at 38.2°, 44.3°, 64.6°, 77.6° and 81.7° with a lattice parameter of 4.080 Å and average particle size of 6.5 nm. Crystalline planes of AuAg-based material are observed in Fig. 1b and located at 38.0°, 44.2°, 64.4°, 77.3° and 82°. The value of lattice parameter is 4.089 Å and average particle size of 21 nm. The observed peaks are characteristic of a single face-centered-cubic (fcc) crystallographic structure of Au (JCPDS 04-0784). Variation of lattice parameter value suggests the presence of electronic interactions between outer electron shells of Ag and Au atoms, reducing the size of Ag atom [18]. This is an indicative of the formation of one phase in the material.

AuAg/C composition was estimated by XRF analysis, Au in 44.4 wt.% and Ag in 55.6 wt.% (0.30 and 0.70 molar ratio, respectively).

XPS results for AuAg nanoparticles are shown in Fig. 2. The binding energies of Au are 84.5 eV ($4f_{7/2}$) and 88.3 eV ($4f_{5/2}$), while for Ag are 368.6 eV ($3d_{5/2}$) and 374.6 eV ($3d_{3/2}$). According with Lubarda these binding energy values correspond to zero-oxidation state [19]. The results suggest the possible formation of AuAg alloy.

SEM images presented in Fig. 3a and b show the presence of Au and AuAg nanoparticles on Vulcan surface, respectively. Both images reveal good dispersion of metallic nanoparticles on Vulcan surface with relative narrow particle size distribution.

3.2. Electrochemical evaluation of AuAg/C and Au/C

Fig. 4 compares the electrochemical responses of Au/C and AuAg/C in 0.3 M KOH measured in the potential range between −750 and 750 mV vs. NHE. The comparison of both voltammetric profiles shows some differences. For AuAg/C electrocatalyst are not observed the peaks corresponding to Ag oxides reduction, this fact supports the idea that the bimetallic material are composed by a solid solution [20].

Electrocatalytic properties of Au/C and AuAg/C for glucose oxidation reaction were investigated in 0.01 M glucose + 0.3 M KOH aqueous solution by cyclic voltammetry. Fig. 5 compares the electrochemical responses measured at 20 mV s^{-1} between −750 and 750 mV vs. NHE. The peaks associated with the glucose oxidation process were recorded in both forward and reverse scans [21]. The onset potential for glucose electrooxidation on AuAg/C electrocatalyst showed a negative shift ca. 150 mV compared with Au/C. The first peak observed in −225 and −380 mV vs. NHE for Au/C and AuAg/C respectively, is related with the transfer of two electrons to form gluconic acid or similar species. The second peak is attributed to successive oxidations of organic molecules [21,22].

Above result indicates that AuAg/C electrocatalyst favors the glucose electrooxidation as compared to Au/C. This behavior could be attributed to the interaction between bimetallic material and glucose. Yet, the mechanism of glucose oxidation involves adsorption of OH^- ions and according to Marichev this process is facilitated on Ag surfaces [23].

Furthermore, in Fig. 5 can be seen that the maximum current density associated with glucose electrooxidation on Au/C and AuAg/C is 1.5 and 3.75 mA cm^{-2} (at 150 mV vs. NHE) respectively.

3.3. Microfluidic fuel cell evaluation

Fig. 6 compares the polarization and power density curves of LMMFC that uses glucose as fuel, equipped with Au/C and AuAg/C as anode electrodes. OCP recorded with Au/C is slightly higher than that obtained with AuAg/C (0.6 V and 0.55 V respectively). The same tendency is followed by the power density: 0.52 and 0.32 mW cm^{-2} (40% less power density with AuAg/C), although the Au loading is 4 times less in AuAg/C material than Au/C.

Fig. 7 compares the power density curves normalized by Au loading. By using of AuAg/C as anode electrode was obtained 2.5 times higher power density than that reached when Au/C was used as anode, confirming the increment of Au activity attributed to the interaction with Ag.

In order to increase the power density and evaluate the stability of LMMFC at high current densities, glucose concentration in

the cell was increased from 0.01 M to 0.05 M (shown for AuAg/C anode electrode). The polarization and power density curves are presented in Fig. 8, where can be seen that maximum power density is near to 0.4 mW cm^{-2}, almost 25% higher than that value obtained with 0.01 M glucose.

Chronoamperometry experiments at 320 mV were carried out in the presence of 0.05 M glucose in 0.3 M KOH aqueous solution for 4 h. Fig. 9 shows the current density behavior for the glucose oxidation as a function of the time. It can be observed that the current density decreases in an exponential way and remains practically constant. This result demonstrates that AuAg/C electrode has electrocatalytic stability for the glucose oxidation reaction under LMMFC operation conditions.

4. Conclusions

In summary Au/C and AuAg/C were synthesized by chemical reduction and physicochemically characterized by XRD, XRF, XPS and SEM techniques. XPS corroborated the presence of Au and Ag in zero oxidation state, suggesting the formation of AuAg alloy. The electrocatalytic properties of the synthesized materials were evaluated for the glucose electrooxidation. AuAg/C exhibits good stability in basic media and higher current density and more negative anodic potential (ca. 150 mV) associated with this reaction than that achieved with Au/C electrocatalysts. This increment in the activity of Au nanoparticles is attributed to the presence of Ag, suggesting the formation of alloying material.

The performance of AuAg/C and Au/C was evaluated in glucose-LMMFC, where the incorporation of Ag in the electrocatalyst, contributes to increasing the AuAg/C activity using low Au loading. Further work is carried out in order to describe the glucose oxidation mechanism in AuAg/C electrode material.

Acknowledgments

The authors thank to the Mexican Council for Science and Technology CONACYT for financial support through Fomix-Chihuahua (grant CHIH-2009-C02-127461). We also thank to CNR-ITAE Institute (Messina, Italy) for support with XRF and XPS measurements. F.M. Cuevas-Muñiz also acknowledges to CONACYT for a graduate scholarship.

References

[1] D. Morales-Acosta, J. Ledesma-García, L.A. Godinez, H.G. Rodríguez, L. Álvarez-Contreras, L.G. Arriaga, J. Power Sources 195 (2010) 461.
[2] R.L. Arechederra, B.L. Treu, S.D. Minteer, J. Power Sources 173 (2007) 156.
[3] D. Morales-Acosta, L.G. Arriaga, L. Alvarez-Contreras, S. Fraire Luna, F.J. Rodríguez Varela, Electrochem. Commun. 11 (2009) 1414.
[4] M. Guerra-Balcázar, D. Morales-Acosta, F. Castañeda, J. Ledesma-García, L.G. Arriaga, Electrochem. Commun. 12 (2010) 864.
[5] S. Calabrese Barton, J. Gallaway, P. Atanassov, Chem. Rev. 104 (2004) 4867.
[6] S. Kerzenmacher, J. Ducrée, R. Zengerlea, F. von Stetten, J. Power Sources 182 (2008) 1.
[7] M. Tominaga, T. Shimazoe, M. Nagashima, I. Taniguchi, Electrochem. Commun. 7 (2005) 189.
[8] L.D. Burke, P.F. Nugent, Gold Bull. 31 (1998) 39.
[9] M. Pasta, R. Ruffo, E. Falletta, C.M. Mari, C. Della Pina, Gold Bull. 43 (2010) 60.
[10] H. Quan, S.-U. Park, J. Park, Electrochim. Acta 55 (2010) 2232.
[11] J. Lin, C. He, Y. Zhao, S. Zhang, Sensor. Actuators B: Chem. 137 (2009) 768.
[12] M. Tominaga, T. Shimazoe, M. Nagashima, I. Taniguchi, J. Electroanal. Chem. 615 (2008) 51.
[13] S.B. Aoun, Z. Dursun, T. Koga, G.S. Bang, T. Sotomura, I. Taniguchi, J. Electroanal. Chem. 567 (2004) 175.
[14] E. Kjeang, N. Djiali, D. Sinton, J. Power Sources 186 (2009) 353.
[15] D. Morales-Acosta, H.G. Rodríguez, L.A. Godinez, L.G. Arriaga, J. Power Sources 195 (2010) 1862.
[16] M. Brust, M. Walker, D. Bethell, D.J. Shiffrin, R. Whyman, J. Chem. Soc. Chem Commun. 7 (1994) 801.
[17] J.L. Cohen, D.J. Volpe, D.A. Westly, A. Pechenik, H.D. Abruña, Langmuir 21 (2005) 3544.
[18] N.N. Kariuki, J. Luo, M.M. Maye, S.A. Hassan, T. Menard, H.R. Naslund, Y. Lin, C. Wang, M.H. Engelhard, C.-J. Zhong, Langmuir 20 (2004) 11240.
[19] V.A. Lubarda, Mech. Mater. 35 (2003) 53.
[20] M. Tominaga, T. Shimazoe, M. Nagashima, H. Kusuda, A. Kubo, Y. Kuwahara, I. Taniguchi, J. Electroanal. Chem. 590 (2006) 37.
[21] M. Tominaga, M. Nagashima, K. Nishiyama, I. Taniguchi, Electrochem. Commun. 9 (2007) 1892.
[22] M. Tominaga, M. Nagashima, K. Nishiyama, I. Taniguchi, Electrochem. Commun. 7 (2005) 189.
[23] V.A. Marichev, Electrochim. Acta 43 (1998) 2203.